Numerical Simulation of Rayleigh Bénard Convection in an Enclosure: Effect of Vibrating Side Wall

Semih CETINDAG, Murat K. AKTAS

***Abstract*—Transient convective heat transfer in an air-filled shallow enclosure with a vibrating side wall is investigated numerically. Rayleigh Bénard convection and oscillatory flows has been the subject of many investigations by using both experimental and theoretical methods. To our best knowledge, the influence of vibrating side wall on classical Rayleigh-Bénard convection has not been studied. In the present study, periodic vibration of the enclosure side wall is employed as a driving force of fluid motion. The sidewalls of enclosure are kept in adiabatic conditions while the bottom wall is isothermally heated and the top wall is kept at initial temperature. A control-volume method based, explicit time-marching Flux-Corrected Transport Algorithm is implemented to solve the fully compressible form of the Navier-Stokes and energy equations. The numerical results of a test case simulation with stationary sidewalls are compared with the existing literature for code validation. The oscillatory fluid motion significantly changes the transient behavior of the thermal transport in the enclosure compared to the pure Rayleigh-Bénard convection.**

***Index Terms*—Compressible flow, Rayleigh-Bénard convection, oscillatory flow**

I. Introduction

Since Bénard's experiment [1] on the convective heat transfer in a thin horizontal layer heated from below and the following theoretical studies of Lord Rayleigh [2], Rayleigh-Bénard convection in confined enclosures has been the subject of many theoretical, experimental and numerical studies due to the great importance it has in various fields of science and engineering. In addition to its applications in varying engineering fields, a great effort has been dedicated Rayleigh-Bénard convection to investigate fluid dynamics instability and chaotic behavior in fluids.

In Rayleigh-Bénard convection, for the implemented no-slip boundary conditions to the walls, before Ra_{cr}= 1707.76 the flow is stationary and the transmission of the heat is only due to the conduction mechanism. The pioneering investigations about this value of the critical Rayleigh number for rigid-rigid and rigid-free boundary conditions were performed by Pellew and Southwell [3] using linear analysis. It has also been determined both analytically by Davis [4] and experimentally by Stork and Muller [5].

Manuscript received April 10, 2014; revised April 12, 2014.

Semih CETINDAG is with TOBB University of Economics and Technology, Ankara, 06560 TURKEY (phone: +90-312-2924086; e-mail: scetindag@etu.edu.tr).

Murat K. AKTAS is with TOBB University of Economics and Technology, Ankara, 06560 TURKEY (e-mail: maktas@etu.edu.tr).

The first studies of nonlinear Rayleigh-Bénard convection and the consequences of surface tension effects had been outlined by Chandrasekhar [6]. When the Rayleigh number increases beyond this critical value (1707.76), convective flows can be observed. In this regime, the fluid motion is regular and organized as a set of horizontal parallel rolls. Moreover, as the Rayleigh number increases, a bifurcation and the second transition from steady to oscillatory flow is observed by Stella and Bucchignani [7]. For a three-dimensional, incompressible flow heated from below, bifurcation patterns for different Prandtl numbers were investigated numerically by Bucchignani and Stella [8]. In this study, they also examined the transition from oscillatory behavior to the chaotic behavior for the same geometry and flow characteristics. In these two studies, incompressible Newtonian fluid was analyzed by employing the Boussinesq approximation. Soong et.al [9] performed the numerical investigations in a two-dimensional, heated from below and cooled from above inclined enclosure for the aspect ratios of 4, 3 and 1. In this study, finite-volume method is used, thermo-physical properties of the fluid were assumed to be constant and Boussinesq approximation was utilized for the gravitation term.

Most of the studies existing in literature are based on Boussinesq approximation for liquid or gas media in order to obtain relatively simple form of the governing equations. However, the range in which this assumption is valid is rather limiting. Gray and Giorgini [10] conducted a study to analyze the validity of the Boussinesq approach for air and water at atmospheric conditions (P=1 atm). In this study, it was concluded that Boussinesq approximation is not a suitable assumption for the relatively higher temperature differences (as low as 2 ℃ for water) and in this case the compressible form of the Navier-Stokes equations has to be used.

The main emphasis of this paper is investigating the transient convective heat transfer in an air-filled shallow enclosure with a vibrating sidewall. Due to the fact that non-Boussinesq effects arise in a wide range of circumstances, instead of considering fluid density to be independent of pressure (i.e., incompressibility assumption) and depend linearly on temperature, it is of interest to use fully compressible equations in the present paper. For the verification of the implemented numerical procedure, stationary wall test cases (i.e., pure Rayleigh- Bénard convection) are used. The achieved numerical results for the test case display a good agreement with the literature. Flow structure and corresponding temperature distribution under the

ISBN: 978-988-19253-5-0
ISSN: 2078-0958 (Print); ISSN: 2078-0966 (Online)

effect of oscillatory motion significantly differs from the pure Rayleigh-Bénard convection which yields to significant augmentation of the heat transfer from the bottom wall.

II. FORMULATION OF THE PROBLEM

A. Problem Geometry

A two-dimensional shallow enclosure filled with air is considered (Fig. 1). The enclosure height is 15 mm and the length is 60 mm. Corresponding aspect ratio (AR) of the enclosure is 4. Air is heated from the below by T_h temperature and cooled from above by T_c temperature and the vertical walls of enclosure are adiabatic.

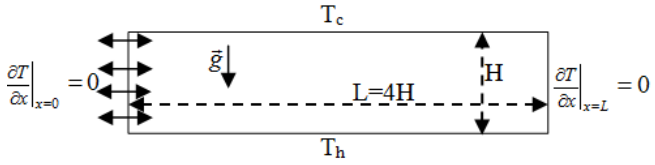

Fig. 1. Problem schematic and corresponding boundary conditions.

No-slip boundary condition was implemented for all solid walls. The oscillatory motion of air is driven by the harmonic vibration of the left wall at certain frequency. The frequency of wall is chosen as to create a standing wave at the first fundamental mode in the enclosure in order to maximize the pressure wave amplitudes and oscillatory flow velocities.

In the simulation of the oscillatory flow and Rayleigh-Bénard convection, the left wall of the enclosure is harmonically vibrated by the formula of

$$X = X_{max}\sin\omega t \tag{1}$$

In the present study, ω (angular frequency) is selected as 18177 rad/s (f= 2893 Hz) and the maximum wall displacement is selected as 5μm, 3μm, 1μm, 0.5μm, 0.4μm, 0.3μm and 0.2μm.

B. Mathematical Model

The compressible form of the Navier-Stokes and the energy equations in Cartesian coordinate system were used in this study to model the interaction of oscillatory flow and Rayleigh-Bénard convection:

Continuity Equation

$$\frac{\partial \rho}{\partial t}+\frac{\partial(\rho u)}{\partial x}+\frac{\partial(\rho v)}{\partial y}=0 \tag{2}$$

Momentum Equations

$$\rho\frac{\partial u}{\partial t}+\frac{\partial P}{\partial x}+\rho u\frac{\partial u}{\partial x}+\rho v\frac{\partial u}{\partial y}-\frac{\partial \tau_{xx}}{\partial x}-\frac{\partial \tau_{xy}}{\partial y}=0 \tag{3}$$

$$\rho\frac{\partial v}{\partial t}+\frac{\partial P}{\partial y}+\rho u\frac{\partial v}{\partial x}+\rho v\frac{\partial v}{\partial y}-\frac{\partial \tau_{yy}}{\partial y}-\frac{\partial \tau_{xy}}{\partial x}+\rho g=0 \tag{4}$$

Energy Equation

$$\frac{\partial E}{\partial t}+\frac{\partial}{\partial x}\left[u(E+P)\right]+\frac{\partial}{\partial y}\left[v(E+P)\right] -\frac{\partial}{\partial x}\left[u\tau_{xx}+v\tau_{xy}\right]-\frac{\partial}{\partial y}\left[u\tau_{xy}+v\tau_{yy}\right]+\frac{\partial q_x}{\partial x}+\frac{\partial q_y}{\partial y}=0 \tag{5}$$

The ratio of specific heats

$$\gamma = C_p/C_v \tag{6}$$

The total energy term

$$E=\frac{P}{\gamma-1}+0.5\rho\left(u^2+v^2\right) \tag{7}$$

Heat flux components for the x and y direction in the Cartesian coordinates is expressed as

$$q_x=-k\frac{\partial T}{\partial x} \quad \text{and} \quad q_y=-k\frac{\partial T}{\partial y} \tag{8}$$

Corresponding stress tensor components in the momentum and energy equation are

$$\tau_{xx}=\frac{4}{3}\mu\frac{\partial u}{\partial x}-\frac{2}{3}\mu\frac{\partial v}{\partial y} \tag{9}$$

$$\tau_{yy}=\frac{4}{3}\mu\frac{\partial v}{\partial y}-\frac{2}{3}\mu\frac{\partial u}{\partial x} \tag{10}$$

$$\tau_{xy}=\mu\left(\frac{\partial u}{\partial y}+\frac{\partial v}{\partial x}\right) \tag{11}$$

Density and temperature variations are related to pressure by the ideal gas law:

$$p=\rho RT \tag{12}$$

where R (=0.287 kJ/kg K) is the gas constant of air.

Initially, pressure (101.325 Pa), temperature (300 K), and density (1.1768 kg/m^3) have uniform values in the enclosure.

C. Numerical Approach

The stated equations in the previous section were solved by using a finite-volume based explicit time marching flux corrected transport (FCT) algorithm. The reason behind using this algorithm for the numerical simulations lies in the fact that it has relatively higher ability to resolve steep gradients with minimum numerical diffusion. FCT is a high-order, nonlinear, monotone, conservative and positivity-preserving method designed to solve a general one-dimensional continuity equation with appropriate source terms. The diffusion terms (the viscous term in the momentum equations and the conduction terms in the energy equation) were discretized using a second-order central difference approach. Time-step splitting was also used to couple all of the representative physical effects. A more detailed discussion of FCT algorithm is performed by Oran and Boris [11]. As stated in the study of Tillet et al. [12], higher order, non-dissipative algorithms such as FCT, requires a great vigilance to prevent the spurious wave reflections in the vicinities of boundaries and nonphysical numerical oscillations arising from instabilities when the boundary conditions are being implemented. In present study, treatment proposed by Poinsot and Lele [13] is used to accurately compute the density along the stationary no-slip walls. Since an algorithm based on explicit numerical method is employed, the CFL (Courant-Friedrichs-Lewy) stability condition is important. In order to satisfy the stability

ISBN: 978-988-19253-5-0
ISSN: 2078-0958 (Print); ISSN: 2078-0966 (Online)

criteria the time step size of the computations was chosen based on

$$\Delta t = (CFL) \times \left[\frac{\min(\Delta x, \Delta y)}{a_{i,j}} \right] \quad (13)$$

The selected CFL number for the analysis is 0.4 which is already smaller than the necessary value of 0.5.

In the present numerical simulations typically 201 x 51 uniform numerical meshes are utilized to be small enough considering the computational time constraint for the enclosure having the height of 15 mm and length of 60 mm, respectively. The computations performed using even denser numerical mesh did not alter the results significantly.

III. RESULTS

For the code validation purpose, the pure Rayleigh-Bénard convection predictions of Soong et al. [9] were used. In the aforementioned study, for AR=4 and Ra=5000, the bottom and the top wall temperatures was taken as T_h=320 K and T_c=300 K, respectively ($\Delta T = 20K$). The dimensionless maximum velocity components u and v and Nu number was compared with the existing data.

For the comparison of these parameters, length and velocity components are non-dimensionalized by H and α/H respectively. Nusselt number is calculated as

$$Nu = \frac{\left(\frac{\partial T}{\partial y}\right)_{ave.} \times H}{\Delta T} \quad (14)$$

TABLE I
COMPARISONS OF THE PRESENT RESULTS WITH THE LITERATURE

	Soong et al. [9]	Present Study
u_{max}	16.1	16.2
v_{max}	18.0	19.7
Nu	2.1	2.12

The present numerical predictions agree quite well with literature. Soong et al. [9] employed Boussinesq approximation in their work. Since fully compressible formulation is employed in the present work v_{max} value slightly differs from the prediction of Soong et al.

Fig. 2 and Fig.3 depict the time evolution of the flow field and temperature distribution at different instants for the case of pure Rayleigh-Bénard convection. The flow field and the corresponding temperature distribution are consistent with the literature.

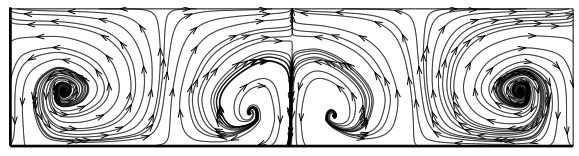

(a)

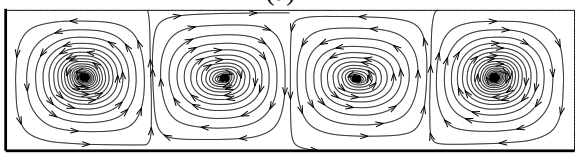

(b)

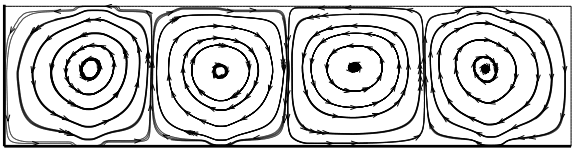

(c)

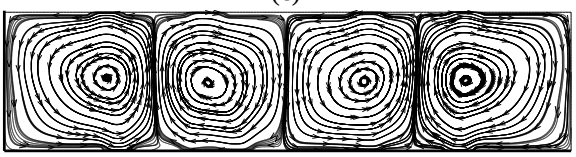

(d)

Fig. 2. Streamlines of different instants for pure Rayleigh-Bénard convection (a) t=0.5 s, (b) t=1 s, (c) t=2.5 s, (d) t=5 s.

At relatively early times (0.5 s) the velocity values are rather small while the plume formation is observed instead of the characteristic nature of the Rayleigh-Bénard cells for AR=4 (Fig. 2a). In the process of time (1 s.), first of all, the characteristic Rayleigh-Bénard cells with relatively small velocity magnitudes starts to be established (Fig. 2b). At 2.5s., the typical cell structure develops but the velocity values continue to increase further (Fig. 2c). At 5 s., the typical cell structure (Ra=5000) with two clock wise and two counter clock wise rotating vortices fully develops (Fig. 2d).

The time evolution of the temperature distribution in the flow domain for pure Rayleigh-Bénard convection was presented in Fig.3. The diffusive transport dominates temperature field at early times (Fig. 3a) and (Fig. 3b). At 2.5 s., the characteristic temperature distribution in Rayleigh-Bénard for AR=4 starts to be established (Fig. 3c). At 5 s., fully developed Rayleigh- Bénard convection cells are observed (Fig. 3d). The fully developed temperature field completely agrees with the results in the literature.

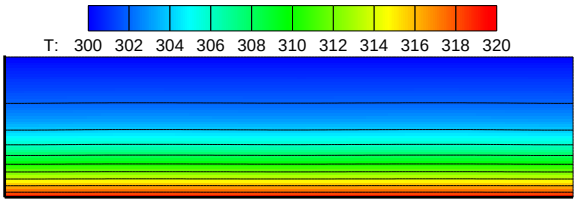

(a)

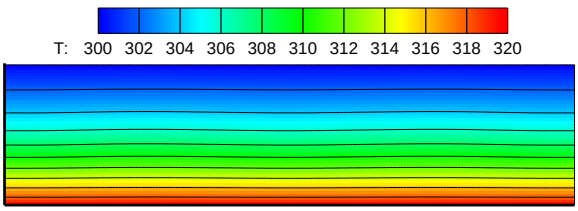

(b)

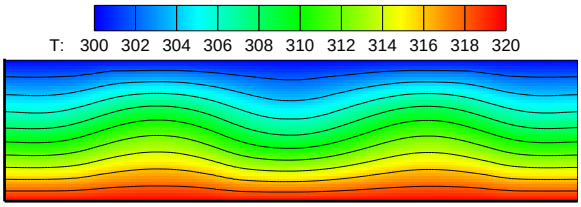

(c)

ISBN: 978-988-19253-5-0
ISSN: 2078-0958 (Print); ISSN: 2078-0966 (Online)

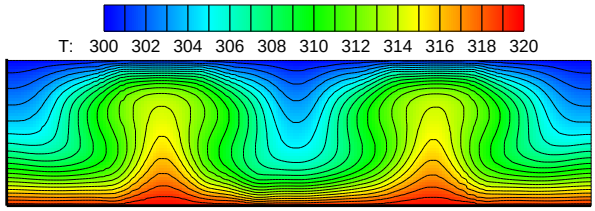

(d)

Fig. 3. Temperature distributions of different instants for pure Rayleigh-Bénard convection (a) t=0.5s, (b) t=1s, (c) t=2.5s, (d) t=5s.

As a secondary validation study of the numerical scheme utilized, pure oscillatory flow is considered for an unheated enclosure. The vibration frequency of the harmonic vibration of the enclosure left wall is chosen as f= 2893 Hz. Four different left wall maximum displacement values were considered. As a rule of thumb, particle velocity (velocity amplitude) should be equal to ratio of the pressure to specific acoustic impedance (Δp/Z), Beranek [14].

Table 2 compares the theoretically calculated maximum velocity values (3rd line) and the maximum velocity predictions of the present numerical study (4th line) for different wall displacements (1 μm, 0.5 μm, 0.3 μm, 0.2 μm).

TABLE II
THEORATICAL AND NUMERICALLY CALCULATED PARTICLE VELOCITY VALUES FOR DIFFERENT WALL DISPLACEMENTS

X_{max}	1 μm	0.5 μm	0.3 μm	0.2 μm
$\Delta P_{left\ wall}$ (Pa)	580	210	117	100
$\Delta P_{left\ wall}/Z$ (m/s)	1.404	0.508	0.281	0.242
$v_{particle}$ (m/s)	1.401	0.501	0.280	0.230
Error (%)	0.214	1.378	0.356	4.956

In the calculation, the specific acoustic impedance is taken as Z=413 (Ns/m^3) for the air of T=20 ^{0}C. The results of the present simulation with theoretical values agree well.

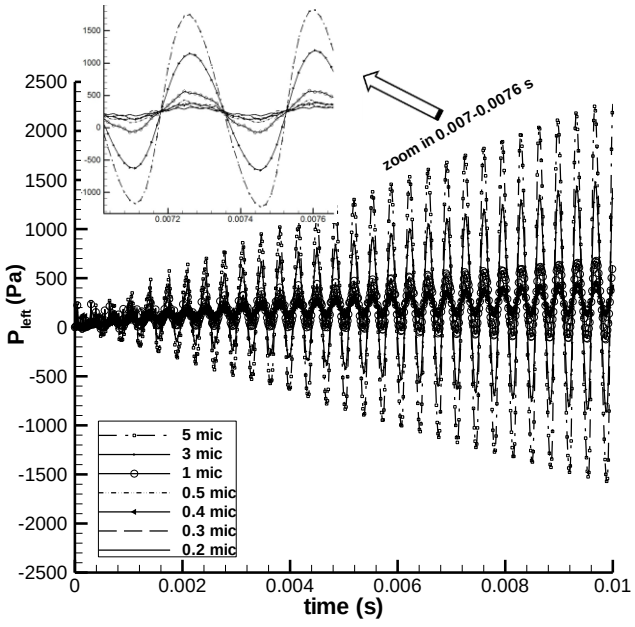

(a)

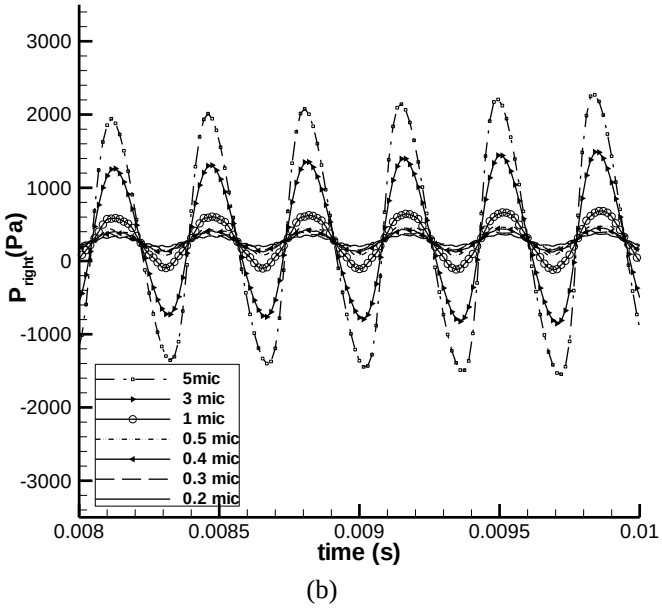

(b)

Fig. 4. Time evolution of relative pressure wave amplitudes for different wall displacement values at the vicinity of t=0.01 (a) on the left wall, and at the vicinity of t=0.01 (b) on the right wall.

The time averaged flow fields in the enclosure at 5 s are shown in Fig. 5 for different cases. At this time, the time averaged velocities reach pseudo-steady values. The time averaging is applied to instantaneous velocity values for one period of wall vibration and pseudo-steady velocity values are obtained.

In Fig. 5a, the signature of flow field is quite similar to that of pure Rayleigh-Bénard convection except the rotation direction of the cells. This pattern indicates a stronger flow field (due to oscillatory wall motion) which has similar to Bénard cells but has opposite flow direction for this amount of wall displacement value.

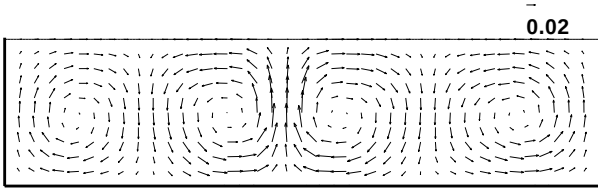

(a)

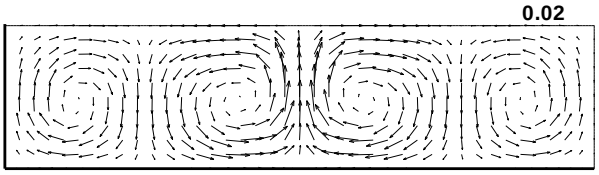

(b)

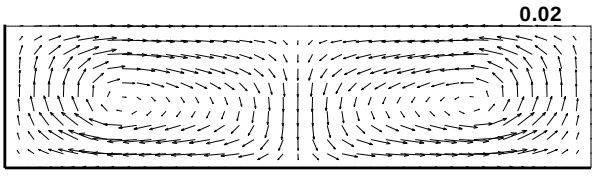

(c)

ISBN: 978-988-19253-5-0
ISSN: 2078-0958 (Print); ISSN: 2078-0966 (Online)

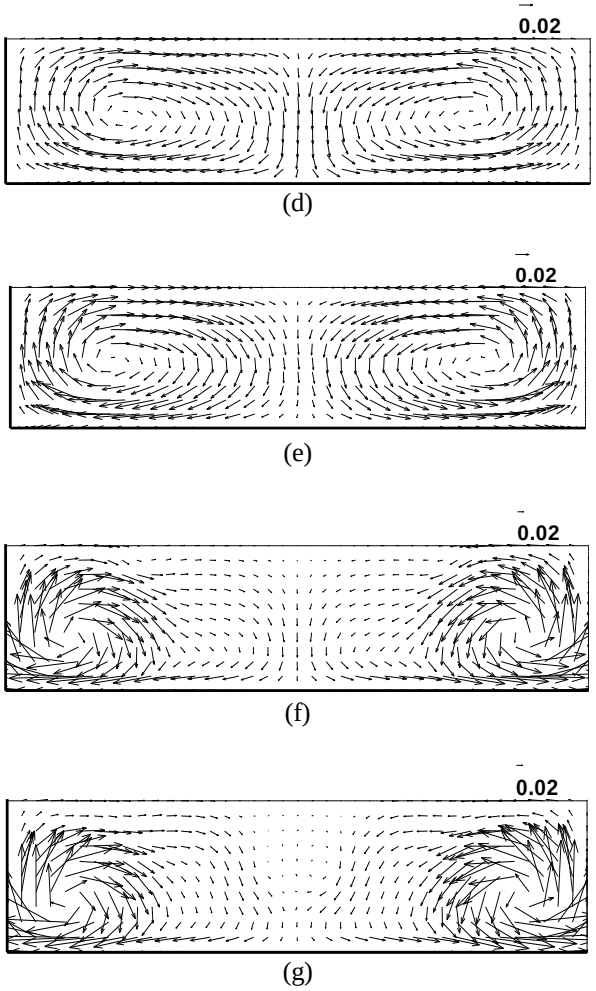

Fig. 5 Cycle averaged velocity vectors for different wall displacement values (a) X_{max}=0.2μm, (b) X_{max}=0.3μm, (c) X_{max}=0.4 μm, (d) X_{max}=0.5 μm, (e) X_{max}=1μm, (f) X_{max}=3μm, (g) X_{max}=5 μm.

Fig.5 shows that below the wall displacement value 0.3 μm, the flow field significantly changes. Because of this alteration in the flow field, Nusselt number for these X_{max} values significantly lower than the higher X_{max} values explained in the Table 3 below.

Table 3 presents the Nusselt numbers from the bottom wall for these different maximum left wall displacement values.

TABLE III
BOTTOM WALL NUSSELT NUMBERS FOR DIFFERENT WALL DISPLACEMENTS

Wall displacement	Cycle averaged Nu number for the bottom wall at 5 s
5 μm	13.82
3 μm	9.57
1 μm	4.29
0.5 μm	3.99
0.4 μm	3.75
0.3 μm	2.67
0.2 μm	2.50
Pure Rayleigh-Benard	2.12

Table 3 lists the cases studied with different maximum wall displacements. The heat transfer values from the bottom wall were calculated using the temperature values of the last vibration cycle. It can be concluded that with increasing wall displacement, heat transfer increases compare to pure Rayleigh- Bénard convection.

IV. CONCLUSIONS

Vibrations are known to be among the most effective ways of enhancing heat transfer due to its pronounced effect on the behavior and stability of fluid systems. The present work is devoted to investigate the effect of left wall of an enclosure on classical Rayleigh-Benard convection numerically.

It is observed that with the increment in the left wall vibration, the flow field significantly differs from the classical Rayleigh-Benard convection cell structure and as a result of this; flow inside the enclosure apt to generate a secondary circulating motions. Furthermore, the last cycle averaged bottom wall Nusselt values increases proportional to the left wall displacements. It is observed that while the classical Rayleigh-Benard convection has a bottom Nu value of 2.116 (Ra=5000), when 5 μm amplitude of vibration is applied to the system, this value increases to 13.821 which is about the 7 times higher than the original value.

REFERENCES

[1] Benard H., Les tourbillons cellularies dans une nappe liquide. Rev. Gen. Sciences Pure Appl., vol. 11, pp.1261-1271, 1900.
[2] Rayleigh L., On convection currents in a horizontal layer of fluid when the higher temperature is on the other side, Phil.Mag., vol. 32, pp. 529-546, 1916.
[3] Pellew, A. Southwell, R.V., On maintained convective motions in a fluid heated from below. Proc. Roy. Soc. London A, vol. 176, 312-343, 1940.
[4] Davis, S., Convection in a Box: Linear Theory, J. Fluid Mech., vol. 30, (3), pp. 465-478, 1967.
[5] Stork K. and U.Muller, Convection in a Box: Experiments, J. Fluid Mech., vol. 54, (4), pp. 599-611., 1972.
[6] Chandrasekhar, S., *Hydrodynamic and Hydromagnetic Stability*. Oxford, Clarendon Press, 1961
[7] Stella F, Bucchignani E., Rayleigh-Benard convection in limited domains: Part 1-Oscillatory Flow, Numerical Heat Transfer, Part A: Applications, vol.36, (1), pp. 1-16, 1999.
[8] Bucchignani E, Stella F., Rayleigh-Benard convection in limited domains: Part 2-Transition to Chaos, Numerical Heat Transfer, Part A: Applications, , vol.36, (1), pp. 17-34, 1999.
[9] Soong C.Y., Tzeng P.Y., Chiang D.C., Sheu T.S., Numerical study on mode-transition of natural convection in differentially heated inclined enclosures, Int. J. Heat Mass Transfer, vol.39, pp. 2869-2882, 1996.
[10] Gray Donald D., Giorgini A., The validity of the Boussinesq approximation for liquids and gases, Int. J. Heat Mass Transfer, vol. 19, pp. 545-551, 1976.
[11] Oran E.S., Boris J. P., *Numerical simulation of reactive Flows*, Cambridge University Press, Cambridge, England, 2000.
[12] Tillet Saint-Martin, X. N. and Oran, E. S., Boundary conditions for FCT based solutions of the Navier-Stokes Equations, pp. 2-7, Navy Research Laboratory, Washington, DC., 1997.
[13] Poinsot T.J., Lele S.K., Boundary conditions for direct simulations of compressible viscous flows, J. Comput. Phys, vol. 101, pp. 104–129, 1992.
[14] Beranek Leo L., *Acoustics*, American Institutes of Physics Inc., Woodbury, New York, 1954.

ISBN: 978-988-19253-5-0
ISSN: 2078-0958 (Print); ISSN: 2078-0966 (Online)